Liu Fei (Orcid ID: 0000-0002-2646-3009)

FAK promotes early osteoprogenitor cell proliferation by enhancing mTORC1 signaling

Shuqun Qi[1, 2], Xiumei Sun[2, 3], Han Kyoung Choi[2], Jinfeng Yao[2, 4], Li Wang[2], Guomin Wu[2, 3], Yun He[2, 5], Jian Pan[1*], Jun-Lin Guan[6], and Fei Liu[2*]

[1]State Key Laboratory of Oral Diseases & National Clinical Research Center for Oral Diseases &Department of Oral and Maxillofacial Surgery, West China Hospital of Stomatology, Sichuan University, Chengdu, Sichuan 610041, China.

[2]Department of Biologic & Materials Sciences and Prosthodontics, University of Michigan School of Dentistry, Ann Arbor, MI 48109, USA

[3]Department of Orthodontics, Jilin University School and Hospital of Stomatology, Changchun, Jilin 130021, China

[4]Department of Stomatology, The Second People's Hospital of Shenzhen, China

[5]Dental Department, College of Medicine, Chengdu University, Chengdu, Sichuan 610075, China

[6]Department of Cancer Biology, University of Cincinnati College of Medicine, Cincinnati, OH 45267, USA

Running title: FAK regulates mTORC1 signaling

* Corresponding author.

Primary correspondent: Fei Liu, DDS, PhD
1011 N University Ave
Department of Biologic and Materials Sciences and Prosthodontics
University of Michigan, School of Dentistry
Ann Arbor, MI
(734)-936-0911

This is the author manuscript accepted for publication and has undergone full peer review but has not been through the copyediting, typesetting, pagination and proofreading process, which may lead to differences between this version and the Version of Record. Please cite this article as doi: 10.1002/jbmr.4029

feiliu@umich.edu

Supplemental data have been included with the submission

Disclosure

All authors state that they have no conflict of interest.

Abstract

Focal adhesion kinase (FAK) has important functions in bone homeostasis but its role in early osteoprogenitor cells is unknown. We show herein that mice lacking FAK in *Dermo1*-expressing cells exhibited low bone mass and decreased osteoblast number. Mechanistically, FAK-deficient early osteoprogenitor cells had decreased proliferation and significantly reduced mammalian/mechanistic target of rapamycin complex 1 (mTORC1) signaling, a central regulator of cell growth and proliferation. Furthermore, our data showed that the pharmacological inhibition of FAK kinase-dependent function alone was sufficient to decrease the proliferation and compromise the mineralization of early osteoprogenitor cells. In contrast to the *Fak* deletion in early osteoprogenitor cells, FAK loss in *Col3.6 Cre*-targeted osteoblasts did not cause bone loss, and *Fak* deletion in osteoblasts did not affect proliferation, differentiation, and mTORC1 signaling but increased the level of active proline-rich tyrosine kinase 2 (PYK2), which belongs to the same non-receptor tyrosine kinase family as FAK. Importantly, mTORC1 signaling in bone marrow stromal cells (BMSCs) was reduced if FAK kinase was inhibited at the early osteogenic

differentiation stage. In contrast, mTORC1 signaling in BMSCs was not affected if FAK kinase was inhibited at a later osteogenic differentiation stage, in which, however, the concomitant inhibition of both FAK kinase and PYK2 kinase reduced mTORC1 signaling. In summary, our data suggest that FAK promotes early osteoprogenitor cell proliferation by enhancing mTORC1 signaling via its kinase-dependent function and the loss of FAK in osteoblasts can be compensated by the upregulated active PYK2.

Key words: FAK, mTORC1, osteoprogenitor, osteoblast, PYK2

Introduction

Focal adhesion kinase (FAK) is an intracellular non-receptor tyrosine kinase. Since its discovery,[1] numerous studies have shown critical roles of FAK in cell adhesion, migration, proliferation, and differentiation.[2,3] FAK can function through its kinase-dependent and kinase-independent functions in different cellular processes.[4-6]

Osteoblasts from osteoporotic human bone had decreased FAK activation compared to osteoblasts from non-osteoporotic control,[7] suggesting an important role of FAK in human bone health. However, our understanding of the roles and mechanisms of FAK in regulating bone homeostasis is very limited. To circumvent the embryonic lethality of *Fak* global knockout,[8] *Fak* has been deleted by different osteoblast-targeted *Cre* transgenic mice.[9-11] An earlier study showed that *Fak* deletion in osteoblasts by *Col2.3-Cre* does not affect mouse bone development.[9] Our

recent study showed that *Fak* deletion in *Osterix*-expressing committed osteoblast precursor cells leads to osteopenia in mice.[10]

mTORC1 is a major regulator of protein synthesis,[12] and it controls cell growth and proliferation through two downstream effectors including the ribosomal protein S6 kinases (S6K1 and 2) and the eukaryotic translation initiation factor 4E (eIF4E)-binding proteins (4EBP1, 2, and 3).[13] S6K1 is required for 5'-terminal oligopyrimidine (5'-TOP) mRNA translation. Because ribosomal proteins and translation elongation factors are encoded by 5'-TOP mRNAs, signaling through the phosphorylation of S6K1 via mTORC1 activation promotes ribosomal biogenesis and enhance protein biosynthesis. The ribosomal protein S6 is the best known S6K1 substrate and its phosphorylation status faithfully reflects the S6K1 activity. 4EBP1 is a repressor of translation initiation; upon phosphorylation by mTORC1 activation, 4EBP1 releases from eIF4E, allowing eIF4E to bind with eIF4G to initiate cap-dependent translation.[13]

Dermo1 (*Twist2*)-*Cre* mouse is one of the commonly used transgenic mice to target early osteoprogenitor cells.[14,15] Inactivation of β1-integrin by *Dermo1-Cre* leads to severely impaired skeletal development.[16] Importantly, integrin-mediated cell adhesion to extracellular matrix activates FAK, which is the key component of the signal transduction pathways triggered by integrins.[17-19] To directly determine the role of FAK in early osteoprogenitor cells in bone homeostasis, we generated *Fak* conditional knockout mouse in which *Fak* was deleted by *Dermo1-Cre*. In addition, we used *Col3.6-Cre*[20] to delete *Fak* in osteoblasts. We showed that *Fak* deletion by *Dermo1-Cre* but not by *Col3.6-Cre* led to bone mass decrease that was accounted for by the

decreased cell proliferation and decreased mTORC1 signaling in FAK-deficient early osteoprogenitor cells but not in FAK-deficient osteoblasts.

Materials and Methods

Mice

The floxed *Fak* (*Fak*$^{flox/flox}$), *Dermo1-Cre*, and *Col3.6-Cre*, and Rosa26-RFP (Ai14) mice were described previously.[5,20-22] *Fak*$^{flox/flox}$, *Dermo1-Cre*, and *Col3.6-Cre* mice were backcrossed for at least 8 generations onto a C57BL/6 background. Male *Fak*$^{flox/flox}$ mice were bred with female *Fak*$^{flox/+}$;*Dermo1-Cre* mice to generate *Fak*$^{flox/flox}$ (Control), *Fak*$^{flox/+}$;*Dermo1-Cre* (CHet) and *Fak*$^{flox/flox}$;*Dermo1-Cre* (CKO^{Dermo1}) mice. Male *Fak*$^{flox/flox}$;RFP/RFP mice were crossed with female *Fak*$^{flox/+}$;*Dermo1-Cre* mice to generate *Fak*$^{flox/+}$;*Dermo1-Cre*; Ai14 (hereafter, CHet-RFP) and *Fak*$^{flox/flox}$;*Dermo1-Cre*; Ai14 (hereafter, CKO^{Dermo1}-RFP) mice. Male *Fak*$^{flox/flox}$;*Col3.6-Cre* mice were bred with female *Fak*$^{flox/flox}$ mice to generate *Fak*$^{flox/flox}$ (Control) and *Fak*$^{flox/flox}$;*Col3.6-Cre* (CKO$^{3.6}$) mice. Mice were housed under pathogen-free conditions at 22 ± 2 °C on a 12:12-h light/dark cycle. Mice were euthanized using overdosing carbon dioxide. All the experimental procedures were carried out with the approval of the Institutional Animal Care and Use Committee at the University of Michigan.

MicroCT analysis

Femora and third lumbar vertebra were dissected and analyzed by micro-computed tomography using an eXplore Locus SP (GE Healthcare Pre-Clinical Imaging, London, ON, Canada) as we described previously.[23] The microCT image used for the analysis of vertebra cortical bone area was established 0.63 mm inferior to the end of cranial growth plate (Fig S1). The analyzer was blind to the identification of the samples.

Histomorphometry

Static histomorphometry was performed similarly to what we described previously.[23-25] All parameters were measured according to the Report of the American Society of Bone and Mineral Research Histomorphometry Nomenclature Committee.[26] The analyzer was blind to the identification of the samples.

Bone marrow stromal cells (BMSCs) isolation and culture

BMSCs were collected from 6-week-old mice in the same way as previously described.[10] Briefly, the end of each femur and tibia was cut and cells were flushed using alpha-MEM. Then the cells were cultured in 100-mm dish for 3 days before half change of the basic medium including alpha-MEM medium, 10% fetal bovine serum (FBS), 100 U/ml penicillin and 100 mg/ml of streptomycin, followed by the full medium change on day 7 and every other day afterward. In some experiments, the adherent cells were trypsinized and plated for experiments on day 10.

BMSCs osteogenic differentiation and Histochemical assay

BMSCs isolated from control, CHet and CKO^{Dermo1} mice were seeded in 6-well plate at 1.3×10^7 cells/well and cultured as described above. The osteogenic medium containing 50 mg/ml of ascorbic acid and 10 mM of beta glycerophosphate was used on day 7 and changed every other day afterward. The alkaline phosphatase (ALP) staining and Alizarin red (AR) staining were performed on day 10 and day 21 respectively as previously described.[10] Crystal violet staining was performed on day 10. Briefly, cells were fixed with 100% methanol at -20°C for 15 mins and stained with 0.5% crystal violet solution at room temperature for 15 mins. Image J was used to measure the size of the colony after ALP staining and crystal violet staining. BMSCs collected from control and $CKO^{Col3.6}$ mice were seeded in 12-well plate at 70,000 cells/well after being trypsinized on day 10. After 24 hours, cells were subjected to osteogenic medium that was changed every other day. ALP staining and AR staining were performed on day 7 and day 21 respectively.

FAK kinase inhibitor and FAK/PYK2 dual inhibitor treatment

BMSCs isolated from wild type mice and $CKO^{Col3.6}$ mice were seeded in 6-well plate at 1.3×10^7 cells/well. FAK kinase inhibitor PF-573,228 (# B1523, Apexbio Technology) or FAK/PYK2 dual inhibitor PF-562,271 (# A8320, Apexbio Technology) was added with different doses at different time points every other day. Cell lysates were collected at indicated time points for western blot analysis. ALP staining and crystal violet staining were performed on day 10. Von Kossa staining was performed on day 21. In brief, cells were fixed using 70% ethanol in room temperature for 30

mins, hydrated to dH_2O and then incubated in 5% silver nitrate at 37°C for 1h before being exposed to light for 30 mins.

Proliferation assay

For experiments using control and $CKO^{Col3.6}$ mice, BMSCs were seeded in 12-well plate at 70,000 cells/well after trypsinizing the mesenchymal colonies on day 10. For the experiments using other mice, BMSCs were directly seeded in 12-well plate at 5×10^6 cells/well. Cells were trypsinized and the cell number was counted on day 3 and day 7. Ki67 immunostaining was performed on day 3 and day 7 as previously described.[10] Briefly, cells were fixed with 4% paraformaldehyde and immunostained using anti-Ki67 antibody (# 9129, Cell Signaling Technology).

Western blot

Western blot was performed as previously described.[10] Antibody information is described below. Anti-β-catenin: # 610153 BD Transduction laboratories; anti-Vinculin: # V4505, Sigma-Aldrich; anti-p-PYK2 (Tyr402): # 3291, Cell Signaling Technology; anti-PYK2: # 3292, Cell Signaling Technology; anti-p-FAK (Tyr397): # 3283, Cell Signaling Technology; anti-FAK: #SC-558, Santa Cruz, USA; anti-p-S6 (Ser240/244): # 5364, Cell Signaling Technology; anti-S6: # 2217, Cell Signaling Technology; anti-p-mTOR (Ser2448): # 2971, Cell Signaling Technology; anti-mTOR: # 2972, Cell Signaling Technology; anti-p-4E-BP1 (Thr37/46): # 2855, Cell Signaling Technology;

anti-4E-BP1: # 9452, Cell Signaling Technology; anti-p-AKT (Ser473): # 4060, Cell Signaling Technology; anti-AKT: # 4691, Cell Signaling Technology.

Statistics

For the comparison between two groups, Student's t-test was used. For the comparison in more than two groups, one way ANOVA with Tukey's multiple comparison tests were performed using GraphPad Prism 8.0. For the comparison of two groups in which have two different variables, two way ANOVA with Sidak's multiple comparison tests were performed using GraphPad Prism 8.0.

Results

Deletion of Fak in Dermo1-expressing cells leads to osteopenia in mice

To determine the role of FAK in early osteoprogenitor cells, we deleted *Fak* using *Dermo1-Cre*. *Dermo1-Cre* mice were generated by inserting the *Cre* recombinase gene within the first exon of *Dermo1*, thus resulting in haploinsufficiency.[21] To determine whether *Dermo1* haploinsufficiency affects normal bone development, we analyzed *Dermo1-Cre/+* and littermate wild type mice. Our data showed that *Dermo1* haploinsufficiency did not affect body weight (Fig S2) and bone mass (Fig S3) in both male and female mice. *Fak* deletion in *Dermo1*-expressing cells did not affect the body weight and femoral bone length of male mice and it slightly decreased the body weight without affecting the femoral bone length of female mice at two months of age (Fig S4). To determine the FAK deletion efficiency, western blot was performed using lysates

extracted from femurs of 2-month-old mice. Our data showed that FAK was similarly deleted in male and female mice (Fig S5). MicroCT analysis showed that *Fak* deletion in *Dermo1*-expressing cells led to a significant decrease in femoral trabecular bone mass (Fig 1A-E) and a significant decrease in femoral cortical bone size (Fig 1F-H) in 2-month-old male mice. Because of the concomitant decrease in both total cross-sectional area and marrow area, there was no change in cortical area and thickness in CKO^{Dermo1} male mice (Fig 1I-J). In vertebra, *Fak* deletion led to a significant decrease in both trabecular and cortical bone mass in male mice (Figure S6). However, *Fak* deletion in *Dermo1*-expressing cells did not affect femoral bone mass in 2-month-old female mice although female CKO^{Dermo1} mice showed the similar trend in the decrease of trabecular thickness and total cross-sectional area, and a decrease in marrow area (Figure S7). Our data suggested that this gender difference was not due to the difference in FAK deletion efficiency between male and female CKO^{Dermo1} mice (Fig S5). The reason underlying this gender difference is unclear.

Histomorphometry analysis also showed the decrease of femoral trabecular bone mass in CKO^{Dermo1} male mice (Fig 2A-E), which was accounted for by a significant decrease in osteoblast number and surface without change in osteoclast number and surface (Fig 2F-I). In addition, *Fak* deletion in *Dermo1*-expressing cells did not affect the bone marrow adipocyte number (data not shown).

FAK deletion in Dermo1-expressing cells leads to decreased BMSC proliferation

To elucidate the mechanism responsible for the decreased bone mass and decreased osteoblast number in CKO^{Dermo1} mice, we determined the effect of *Fak* deletion on the proliferation of early mesenchymal lineage cells using primary bone marrow stromal cell (BMSC) culture system. Because of the heterogeneity nature of BMSC culture, first we performed lineage mapping experiments by introducing Rosa26-RFP reporter into CHet and CKO^{Dermo1} mice. BMSCs were isolated from CHet-RFP and CKO^{Dermo1}-RFP mice and the percentage of RFP-positive cells within BMSC colonies were analyzed. Our data showed that there was a significant decrease in the percentage of RFP-positive cells in CKO^{Dermo1}-RFP group compared to CHet-RFP group (Fig 3A-B), suggesting that the *Fak*-deleted BMSCs had compromised ability to increase their number.

To determine the mechanism that was accountable for the decrease in the percentage of RFP-positive cells in CKO^{Dermo1}-RFP group, we performed immunofluorescence staining of Ki67, a proliferation marker. Our data showed that there were significantly less Ki67-positive cells within the RFP-positive cells of CKO^{Dermo1}-RFP group compared to that of CHet-RFP group in day 7 culture while there was no difference between these two groups at day 3 (Fig 3C-D). Consistent with a decrease in proliferation, BMSCs isolated from CKO^{Dermo1} mice had a significant decrease in cell number in day 7 culture (Fig 3E). To determine whether *Dermo1* haploinsufficiency itself affects the BMSC proliferation, we performed similar experiments using BMSCs isolated from *Dermo1*-Cre/+ mice and their wild type littermates. Our data showed that two groups had comparable percentage of Ki67-positive BMSCs and total cell number (Fig S8).

Next, we determined the effect of *Fak* deletion in *Dermo1*-expressing cells on the colony-forming units-fibroblastic (CFU-F) formation. Our data showed CKO^{Dermo1} group had a significant decrease in both CFU-F number and size (Fig 3F-H). Similarly, CKO^{Dermo1} group had a significant decrease in both the number and size of ALP-positive CFU-F (CFU-ALP) (Fig S9A-C). In addition, the CKO^{Dermo1} group had significantly compromised mineralization (Fig S9D-E).

FAK kinase inhibition leads to decreased BMSC proliferation

FAK has both kinase–dependent and–independent functions.[4,27] To determine the contribution of the kinase-dependent function of FAK to the BMSC proliferation, we utilized the specific FAK kinase inhibitor PF-573,228,[28] which is a potent ATP-competitive, reversible inhibitor of FAK kinase activity and was developed to treat various cancers.[29,30] It was shown that PF-573,228 can block >75-80% endogenous FAK activity at the concentration of 0.3-3 μM in different cell types.[28] Thus, we first determined the effect of PF-573,228 on the inhibition of FAK kinase activation at the dose of 0.1 μM to 2 μM. Our data showed that 1 μM PF-573,228 effectively inhibited FAK kinase activation shown by the significantly decreased phospho-FAK^{Tyr397} level (Fig 4A-B). When BMSCs isolated from CHet-RFP mice were treated with 1 μM PF-573,228, there was a significant decrease in the percentage of Ki67-positive cells within the RFP-positive cells (Fig 4C-D) and a significant decrease in total cell number (Fig 4E). Furthermore, PF-573,228 significantly decreased CFU-F number and size (Fig 4F-H), ALP-positive CFU-F number and size (Fig S10A-C) and mineralization (Fig S10D-E) of BMSCs. Thus, our data suggested that the loss

of FAK's kinase-dependent function contributed significantly to the proliferation inhibition in *Fak*-deleted *Dermo1*-expressing BMSCs.

FAK deficiency in Dermo1-expressing cells leads to decreased mTORC1 signaling

To elucidate the molecular mechanism that was responsible for the decreased proliferation in CKO^{Dermo1} BMSCs, we started with determining the effect of *Fak* deletion in *Dermo1*-expressing cells on β-catenin level because we previously showed that *Fak* deletion in *Osterix*-expressing cells leads to a significant decrease in β-catenin level.[10] First, we determined the FAK deletion efficiency in our BMSC cultures. In most of the experiments (5 out of 9) performed, there was sufficient FAK deletion; however, in some experiments (4 out of 9), FAK was not sufficiently deleted (Fig S11A). For cell signaling study, we focused on the five experiments with sufficient FAK deletion. Our data showed that *Fak* deletion in *Dermo1*-expressing cells did not affect β-catenin level (Fig 5A-B). This is unexpected because our previous study showed *Fak* deletion in *Osterix*-expressing cells significantly decreases β-catenin level.[10] Next, we examined the effect of *Fak* deletion in *Dermo1*-expressing cells on the mTORC1 signaling because our previous study suggested that mTORC1 signaling is an important positive regulator on proliferation of osteoprogenitor cells.[31] Our data showed that *Fak* deletion in *Dermo1*-expressing cells significantly inhibited mTORC1 activity demonstrated by the decrease in the level of phospho-mTOR and phospho-S6 (Fig 5A-B). However, there was no change in phospho-4EBP1, the other downstream effector of mTORC1 (Fig 5A-B). In addition, *Fak* deletion in *Dermo1*-expressing

cells significantly decreased phospho-AKT level and there was no change in phospho-PYK2 level (Fig 5A-B). Of note, in the experiments in which FAK was not sufficiently deleted, the levels of phospho-S6 and phospho-AKT were not decreased (Fig S11B), further supporting the connection between FAK and AKT/mTORC1 signaling. To further determine the regulation of mTORC1 activity by FAK in *Dermo1*-expressing BMSCs, we performed immunofluorescence staining using antibody against phospho-S6. Our data showed a similar expression pattern between CHet-RFP and CKO^{Dermo1}-RFP in day 3 culture; however, there was a significant decrease in the percentage of phospho-S6 positive cells within RFP-positive cells in CKO^{Dermo1}-RFP group in day 7 culture (Fig 5C-D).

Fak deletion in osteoblasts does not affect bone development

Our current study and previous study[10] showed that FAK in *Dermo1*-expressing early osteoprogenitor cells and *Osterix*-expressing committed osteoblast precursors plays important role in bone development. To determine the effect of *Fak* deletion in osteoblasts on bone development, we analyzed *Fak* conditional knockout mice targeted by *Col3.6-Cre* ($CKO^{Col3.6}$). In femoral bone of $CKO^{Col3.6}$ mice, FAK was efficiently deleted in association with an increase in phospho-PYK2 level (Fig 6A). $CKO^{Col3.6}$ mice developed normally (Fig 6B). $CKO^{Col3.6}$ male mice had a transient small but statistically significant decrease in body weight during early postnatal growth with similar body length (Fig 6C-D). In addition, *Fak* deletion in osteoblast did not affect the body weight but slightly decreased the body length in $CKO^{Col3.6}$ female mice (Fig S12). Furthermore,

microCT analysis showed that $CKO^{Col3.6}$ male mice had similar trabecular (Fig 6E-H) and cortical (Fig 6I-L) bone parameters compared with control mice. Histomorphometric analysis showed that there were no changes in both osteoblast and osteoclast parameters in $CKO^{Col3.6}$ male mice compared with the controls (data not shown).

Fak deletion in osteoblasts does not affect BMSC proliferation and mTORC1 activity

To further determine the extent that FAK regulates osteoblast function, we performed cellular and signaling studies using BMSCs isolated from $CKO^{Col3.6}$ and control mice. First, our data showed that *Fak* deletion in osteoblasts did not affect the BMSC proliferation evidenced by the similar percentage of Ki67-positive cells (Fig 7A-B) and similar cell number (Fig 7C) in $CKO^{Col3.6}$ group compared to control group. Second, *Fak* deletion in osteoblasts did not compromise the osteogenic differentiation and mineralization of BMSCs (Fig 7D-E). Third, despite the effective FAK deletion, there was no change in the levels of phospho-S6 and β-catenin in $CKO^{Col3.6}$ BMSCs (Fig 7F-G). Notably, there was a significant increase in phospho-PYK2 level in $CKO^{Col3.6}$ group (Fig 7F-G).

The inhibition of mTORC1 signaling by FAK kinase inhibitor is cell differentiation stage-dependent

To elucidate the underlying mechanisms by which FAK was differentially required to support the proliferation and mTORC1 signaling in early osteoprogenitor cells vs. osteoblasts, we turned to the strategy of treating BMSCs with FAK kinase inhibitor at different differentiation stages. First,

we characterized the osteogenic differentiation status of BMSCs in our culture model at different time points. ALP staining showed negative staining at day 3 but wide-spread alkaline phosphatase-positive colonies in day 7 and day 10 cultures (Fig 8A). In addition, we found nearly all cells were negative for Osterix, a marker of committed osteoblast precursor, at the first two days of culture; there were increasingly more and more Osterix-positive cells starting from day 3 and nearly all of them were Osterix-positive at day 7 (data not shown). Next, we designed a treatment regimen using FAK kinase inhibitor to further determine the effect of FAK kinase inhibition on Wnt/β-catenin and mTORC1 signaling at different differentiation stages (Fig 8B). Our data showed that β-catenin level was only consistently inhibited if FAK kinase inhibitor was added when cells started to express Osterix, which was around day 3 in our culture system; on the other hand, AKT and mTORC1 signaling was consistently inhibited when FAK kinase inhibitor was added at earlier culture in cohort I but not later culture in cohort II (Fig 8C-E). Importantly, our data showed that there was a significant increase in phospho-PYK2 level when FAK kinase inhibitor was added in later culture but not in early culture (Fig 8C-E), which was similar to the increase in phospho-PYK2 level observed in BMSCs of $CKO^{Col3.6}$ mice (Fig 7F-G). This suggested that the lack of effect of FAK inhibition in osteoblasts on AKT and mTORC1 signaling was likely due to the compensatory increase in PYK2 activity. Finally, we determined the effect of FAK kinase inhibition at different differentiation stages on BMSC mineralization by von Kossa staining (Fig S13A). Our data showed that early FAK kinase inhibition starting from day 1 or day 3 led to significantly decreased mineralized nodule numbers; however FAK kinase inhibition starting from

day 7 did not decrease BMSC mineralization. Interestingly, the transient FAK kinase inhibition from day 1 to day 7 was sufficient to compromise the later mineralization (Fig S13B-C). Taken together, our data indicated that FAK kinase activity has an important role in early osteoblast lineage cells but not in late osteoblasts.

Dual inhibition of FAK kinase and PYK2 kinase decreases mTORC1 signaling and compromises osteogenic differentiation of BMSCs at later differentiation stage

To test the hypothesis that PYK2 compensates for the loss of FAK at later differentiation stage of BMSCs, we determined the effect of dual inhibition of FAK kinase and PYK2 kinase on mTORC1 signaling by using FAK/PYK2 dual inhibitor PF-562,271[32] at a later differentiation stage of BMSCs. First, our data showed that 1 μM FAK/PYK2 dual inhibitor effectively inhibited the levels of both phospho-FAK^{Tyr397} and phospho-PYK2^{Tyr402} (Fig 9A-C) in wild type BMSCs. Next, the addition of FAK/PYK2 dual inhibitor starting from day 7 BMSC culture significantly decreased the mTORC1 signaling and the level of phospho-AKT in wild type BMSCs (Fig 9D-F). Finally, our data showed that FAK/PYK2 dual inhibitor treatment starting from day 7 culture inhibited osteogenic differentiation and mineralization (Fig S14). This inhibitory effect was absent in FAK inhibitor treatment (Fig S13, D7-D21 group), highlighting the significant difference between these two inhibitors.

To further determine the potential compensatory role of PYK2 when FAK is absent at later differentiation stage of BMSCs, we used the BMSCs isolated from CKO$^{Col3.6}$ mice because our

data showed that PYK2 activity was increased and there was no change in the proliferation and differentiation in $CKO^{Col3.6}$ BMSCs compared to controls (Fig 7). As expected, the addition of FAK/PYK2 dual inhibitor starting from day 7 significantly decreased the p-PYK2 level in $CKO^{Col3.6}$ BMSCs (Fig S15B). Importantly, dual inhibitor treatment decreased the mTORC1 signaling and the level of phospho-AKT in $CKO^{Col3.6}$ BMSCs (Fig S15C-D). Lastly, although $CKO^{Col3.6}$ BMSCs had comparable osteogenic differentiation and mineralization potential compared to control (Fig S16A-B), FAK/PYK2 dual inhibitor treatment starting from day 7 culture inhibited osteogenic differentiation and mineralization in $CKO^{Col3.6}$ BMSCs (Fig S16C-G).

Altogether, our data showed that FAK regulates Wnt/β-catenin signaling and mTORC1 signaling of osteoblast lineage cells in a differentiation stage-dependent manner. FAK kinase inhibition in early osteoprogenitor cells compromised mTORC1 signaling but its inhibition in osteoblasts did not compromise mTORC1 signaling or in vitro mineralization because of the compensation by upregulated active PYK2.

Discussion

We previously showed that *Fak* deletion by *Osterix-Cre* leads to enhanced bone marrow adipogenesis in association with a significant decrease in β-catenin level.[10] In this study we showed that *Fak* deletion by *Dermo1-Cre* or *Col3.6-Cre* did not increase bone marrow adipogenesis nor decreased β-catenin level, indicating the regulation of β-catenin level by *Fak* is cell differentiation stage-dependent. To support this notion, our data showed a significant decrease

in β-catenin level when FAK kinase activity was inhibited by FAK specific kinase inhibitor in BMSCs around the start of Osterix expression but the earlier or later inhibition of FAK kinase activity did not affect β-catenin level. Moreover, an early transient FAK kinase inhibition surprisingly increased β-catenin level; suggesting the complex regulatory mechanism on β-catenin level by FAK. Our previous report also showed that while *Fak* deletion in *Osterix*-expressing cells significantly decreases the β-catenin level in BMSCs but it does not decrease the β-catenin level in more mature calvarial osteoblasts.[10] The underlying mechanism for the differential effects of FAK inhibition at different differentiation stages on β-catenin level remains to be determined.

Through both genetic and pharmacological approaches, we identified a novel regulatory function of FAK on mTORC1 signaling in early osteoprogenitor cells. Our data also showed that FAK positively regulated the phospho-AKT level in these cells. The serine/threonine protein kinase AKT is a downstream effector of PI3K. Because FAK positively regulates PI3K/AKT pathway,[33] and *Fak* overexpression can promote proliferation partly through PI3K/AKT pathway,[34] the proliferation defect in *Fak*-deficient early osteoprogenitor cells is likely contributed by the decrease in AKT signaling. Furthermore, AKT can promote mTORC1 activity by inactivating TSC2,[35,36] and AKT deficiency impairs cell proliferation in mTORC1-dependent manner.[37] Our data showed a concomitant decrease in both AKT and mTORC1 signaling in FAK-deficient cells. Thus, the proliferation defect in the mutant cells is potentially mediated through AKT/mTORC1 axis. AKT can phosphorylate mTOR at Thr2446 and Ser2448;[13] our data showed that FAK inhibition decreased Ser2448 phosphorylation of mTOR, further supporting the notion that FAK may regulate mTORC1 through AKT pathway. It is generally believed that AKT-mediated

mTORC1 regulation applies to both S6K1 and 4EBP1 pathways because both S6K1 phosphorylation and 4EBP1 phosphorylation are significantly decreased in the cells lacking AKT1 and AKT2.[38] However, it has also been reported that knockdown of *Akt*1, 2, and 3 in bladder cancer cell lines specifically decreases S6K1 phosphorylation but not 4EBP1 phosphorylation level.[39] In addition, silencing or pharmacological inhibition of mTOR suppresses S6K1 but not 4EBP1 phosphorylation in the same cancer cell lines.[39] Thus, it was proposed that 4EBP1 phosphorylation is regulated independent of AKT/mTORC1 axis. In our study, FAK-deficient early osteoprogenitor cells had decreased phosphorylation of AKT and mTOR, and mTORC1 signaling was only defective in S6K1 branch but not 4EBP1 branch. This suggests that similar regulatory mechanisms exist in early osteoprogenitor cells compared to the reported bladder cancer cell lines. However, the mechanism of FAK's selective regulation on S6K1 pathway in early osteoprogenitor cells remains to be determined.

In this study, we used *Col3.6-Cre* transgenic mice to target osteoblasts. We previously characterized its expression and activity.[20] A recent study by Rajshankar et al. used this same transgenic mouse to delete *Fak* in osteoblasts and showed very different phenotype from ours. In that study, it was shown that the *Fak* conditional knockout mice are much shorter, have severely crooked and much shorter tails, and have a significant decrease in bone mass.[11] None of these phenotypes was observed in our *Fak* conditional knockout mice using the same *Col3.6-Cre*. There are two potential explanations for these discrepancies. First is the difference in genetic background. The mice used in Rajshankar et al.'s study were B6/CD-1 mixed background and ours had been

backcrossed for at least eight generations onto a C57BL/6 background. Second is the difference in the *Fak* floxed mouse line. Rajshankar et al. used the *Fak* floxed mice generated by Drs. Beggs and Reichardt's group in which LoxP sites flank the second kinase domain exon.[40] In this study, we used the *Fak* floxed mice that we previously generated by flanking the third coding exon which is located at its FERM domain.[5] Cre-mediated deletion of exon 3 leads to a frame-shift mutation and produces a small truncated and nonfunctional peptide.

In this report, we showed that *Fak* deletion in *Dermo1*-expressing early osteoprogenitor cells had defective proliferation due to a decrease in mTORC1 activity. In contrast, *Fak* deletion in osteoblasts had no significant effect on proliferation and differentiation as well as mTORC1 activity. Our data suggested that FAK is dispensable in mature osteoblasts and this is likely due to the compensatory role of PYK2, which belongs to the same non-receptor tyrosine kinase family as FAK[41]. We draw this conclusion because: 1) our data and another study[9] showed an upregulation of PYK2 activity in FAK-deficient osteoblasts; 2) our data showed that FAK/PYK2 dual inhibitor but not FAK inhibitor decreased mTORC1 signaling and inhibited the osteogenic differentiation of BSMCs if added at a later differentiation stage (after the expression of Osterix); and 3) our data showed that *Fak* deletion in osteoblasts using *Col3.6-Cre* did not affect the mTORC1 signaling and differentiation of BMSCs, but the additional inhibition of PYK2 kinase decreased mTORC1 signaling and compromised BMSC differentiation. In addition, a previous study showed that PYK2 knockdown reduces S6K1 expression and phosphorylation in prostate cancer cells.[42]

In summary, our study identified a novel FAK-mTORC1 signaling axis mediated by the kinase-dependent function of FAK in regulating cell proliferation; and this signaling cascade specifically operates in the early osteoprogenitor cells but not in osteoblasts. As a result, *Fak* deletion in early osteoprogenitor cells led to osteopenia in mice but its deletion in osteoblasts did not affect bone development. Altogether, our studies suggested that FAK plays differential roles at different differentiation stages of osteoblast lineage cells: in early osteoprogenitor cells, it promotes the proliferation via positively regulating mTORC1 signaling; in committed osteoblast precursors, it promotes osteoblast proliferation and differentiation via positively regulating both mTORC1 and Wnt/β-catenin signaling; and in osteoblasts, the loss of FAK can be compensated by upregulated active PYK2 (Fig 10).

Acknowledgments

We thank Ms. Andrea Clark for microCT scanning and reconstruction, and Dr. Laurie McCauley for valuable discussion. MicroCT work was partly supported by P30 Core Center award to University of Michigan from NIH/NIAMS (AR 69620). FL was supported by Department of Biologic and Materials Sciences & Prosthodontics, University of Michigan School of Dentistry.

Author's roles: Study design: SQ, XS, HC, JY, LW, JP, JG and FL. Data acquisition: SQ, XS, HC, JY, LW, GW, and YH. Data analysis and interpretation: SQ, XS, JY, LW, GW, YH, JP, JG

and FL. Drafting manuscript: SQ and FL. Approving final version of manuscript: SQ, XS, HC, JY, LW, GW, YH, JP, JG and FL. FL takes responsibility for the integrity of the data analysis.

References:

1. Guan JL, Shalloway D. Regulation of focal adhesion-associated protein tyrosine kinase by both cellular adhesion and oncogenic transformation. Nature. Aug 20 1992;358(6388):690-2. Epub 1992/08/20.
2. Luo M, Guan JL. Focal adhesion kinase: a prominent determinant in breast cancer initiation, progression and metastasis. Cancer Lett. Mar 28 2010;289(2):127-39. Epub 2009/08/01.
3. Schaller MD. Cellular functions of FAK kinases: insight into molecular mechanisms and novel functions. J Cell Sci. Apr 01 2010;123(Pt 7):1007-13.
4. Zhao X, Peng X, Sun S, Park AY, Guan JL. Role of kinase-independent and -dependent functions of FAK in endothelial cell survival and barrier function during embryonic development. J Cell Biol. Jun 14 2010;189(6):955-65. Epub 2010/06/10.
5. Shen TL, Park AY, Alcaraz A, Peng X, Jang I, Koni P, et al. Conditional knockout of focal adhesion kinase in endothelial cells reveals its role in angiogenesis and vascular development in late embryogenesis. J Cell Biol. Jun 20 2005;169(6):941-52.
6. Lim ST, Chen XL, Lim Y, Hanson DA, Vo TT, Howerton K, et al. Nuclear FAK promotes cell proliferation and survival through FERM-enhanced p53 degradation. Mol Cell. Jan 18 2008;29(1):9-22.
7. Perinpanayagam H, Zaharias R, Stanford C, Brand R, Keller J, Schneider G. Early cell adhesion events differ between osteoporotic and non-osteoporotic osteoblasts. J Orthop Res. Nov 2001;19(6):993-1000.
8. Ilic D, Furuta Y, Kanazawa S, Takeda N, Sobue K, Nakatsuji N, et al. Reduced cell motility and enhanced focal adhesion contact formation in cells from FAK-deficient mice. Nature. Oct 12 1995;377(6549):539-44.
9. Kim JB, Leucht P, Luppen CA, Park YJ, Beggs HE, Damsky CH, et al. Reconciling the roles of FAK in osteoblast differentiation, osteoclast remodeling, and bone regeneration. Bone. Jul 2007;41(1):39-51. Epub 2007/04/27.
10. Sun C, Yuan H, Wang L, Wei X, Williams L, Krebsbach PH, et al. FAK Promotes Osteoblast Progenitor Cell Proliferation and Differentiation by Enhancing Wnt Signaling. J Bone Miner Res. Dec 2016;31(12):2227-38.
11. Rajshankar D, Wang Y, McCulloch CA. Osteogenesis requires FAK-dependent collagen synthesis by fibroblasts and osteoblasts. FASEB J. Mar 2017;31(3):937-53.
12. Laplante M, Sabatini DM. mTOR signaling in growth control and disease. Cell. Apr 13 2012;149(2):274-93.

13. Hay N, Sonenberg N. Upstream and downstream of mTOR. Genes Dev. Aug 15 2004;18(16):1926-45.
14. Elefteriou F, Yang X. Genetic mouse models for bone studies--strengths and limitations. Bone. Dec 2011;49(6):1242-54. Epub 2011/09/13.
15. VanKoevering KK, Williams BO. Transgenic mouse strains for conditional gene deletion during skeletal development IBMS BoneKEy. 2008;5(5):151-70.
16. Shekaran A, Shoemaker JT, Kavanaugh TE, Lin AS, LaPlaca MC, Fan Y, et al. The effect of conditional inactivation of beta 1 integrins using twist 2 Cre, Osterix Cre and osteocalcin Cre lines on skeletal phenotype. Bone. Nov 2014;68:131-41. Epub 2014/09/04.
17. Guan JL. Integrin signaling through FAK in the regulation of mammary stem cells and breast cancer. IUBMB Life. Apr 2010;62(4):268-76. Epub 2010/01/27.
18. Guan JL. Focal adhesion kinase in integrin signaling. Matrix Biol. Oct 1997;16(4):195-200. Epub 1997/12/24.
19. Cary LA, Guan JL. Focal adhesion kinase in integrin-mediated signaling. Front Biosci. Jan 15 1999;4:D102-13. Epub 1999/01/16.
20. Liu F, Woitge HW, Braut A, Kronenberg MS, Lichtler AC, Mina M, et al. Expression and activity of osteoblast-targeted Cre recombinase transgenes in murine skeletal tissues. Int J Dev Biol. Sep 2004;48(7):645-53. Epub 2004/10/08.
21. Yu K, Xu J, Liu Z, Sosic D, Shao J, Olson EN, et al. Conditional inactivation of FGF receptor 2 reveals an essential role for FGF signaling in the regulation of osteoblast function and bone growth. Development. Jul 2003;130(13):3063-74.
22. Madisen L, Zwingman TA, Sunkin SM, Oh SW, Zariwala HA, Gu H, et al. A robust and high-throughput Cre reporting and characterization system for the whole mouse brain. Nat Neurosci. Jan 2010;13(1):133-40.
23. Liu F, Fang F, Yuan H, Yang D, Chen Y, Williams L, et al. Suppression of autophagy by FIP200 deletion leads to osteopenia in mice through the inhibition of osteoblast terminal differentiation. J Bone Miner Res. Nov 2013;28(11):2414-30. Epub 2013/05/02.
24. Chandhoke TK, Huang YF, Liu F, Gronowicz GA, Adams DJ, Harrison JR, et al. Osteopenia in transgenic mice with osteoblast-targeted expression of the inducible cAMP early repressor. Bone. Jul 2008;43(1):101-9. Epub 2008/05/08.
25. Choi HK, Yuan H, Fang F, Wei X, Liu L, Li Q, et al. Tsc1 Regulates the Balance Between Osteoblast and Adipocyte Differentiation Through Autophagy/Notch1/beta-Catenin Cascade. J Bone Miner Res. Nov 2018;33(11):2021-34.
26. Dempster DW, Compston JE, Drezner MK, Glorieux FH, Kanis JA, Malluche H, et al. Standardized nomenclature, symbols, and units for bone histomorphometry: a 2012 update of the report of the ASBMR Histomorphometry Nomenclature Committee. J Bone Miner Res. Jan 2013;28(1):2-17. Epub 2012/12/01.

27. Luo M, Zhao X, Chen S, Liu S, Wicha MS, Guan JL. Distinct FAK activities determine progenitor and mammary stem cell characteristics. Cancer Res. Sep 1 2013;73(17):5591-602.
28. Slack-Davis JK, Martin KH, Tilghman RW, Iwanicki M, Ung EJ, Autry C, et al. Cellular characterization of a novel focal adhesion kinase inhibitor. J Biol Chem. May 18 2007;282(20):14845-52. Epub 2007/03/31.
29. Sulzmaier FJ, Jean C, Schlaepfer DD. FAK in cancer: mechanistic findings and clinical applications. Nat Rev Cancer. Sep 2014;14(9):598-610. Epub 2014/08/08.
30. Golubovskaya VM. Targeting FAK in human cancer: from finding to first clinical trials. Front Biosci (Landmark Ed). 2014;19:687-706. Epub 2014/01/07.
31. Fang F, Sun S, Wang L, Guan JL, Giovannini M, Zhu Y, et al. Neural Crest-Specific TSC1 Deletion in Mice Leads to Sclerotic Craniofacial Bone Lesion. J Bone Miner Res. Jul 2015;30(7):1195-205. Epub 2015/02/03.
32. Stokes JB, Adair SJ, Slack-Davis JK, Walters DM, Tilghman RW, Hershey ED, et al. Inhibition of focal adhesion kinase by PF-562,271 inhibits the growth and metastasis of pancreatic cancer concomitant with altering the tumor microenvironment. Mol Cancer Ther. Nov 2011;10(11):2135-45. Epub 2011/09/10.
33. Sonoda Y, Watanabe S, Matsumoto Y, Aizu-Yokota E, Kasahara T. FAK is the upstream signal protein of the phosphatidylinositol 3-kinase-Akt survival pathway in hydrogen peroxide-induced apoptosis of a human glioblastoma cell line. J Biol Chem. Apr 9 1999;274(15):10566-70.
34. Yamamoto D, Sonoda Y, Hasegawa M, Funakoshi-Tago M, Aizu-Yokota E, Kasahara T. FAK overexpression upregulates cyclin D3 and enhances cell proliferation via the PKC and PI3-kinase-Akt pathways. Cell Signal. Jun 2003;15(6):575-83.
35. Inoki K, Li Y, Zhu T, Wu J, Guan KL. TSC2 is phosphorylated and inhibited by Akt and suppresses mTOR signalling. Nat Cell Biol. Sep 2002;4(9):648-57.
36. Manning BD, Tee AR, Logsdon MN, Blenis J, Cantley LC. Identification of the tuberous sclerosis complex-2 tumor suppressor gene product tuberin as a target of the phosphoinositide 3-kinase/akt pathway. Mol Cell. Jul 2002;10(1):151-62.
37. Skeen JE, Bhaskar PT, Chen CC, Chen WS, Peng XD, Nogueira V, et al. Akt deficiency impairs normal cell proliferation and suppresses oncogenesis in a p53-independent and mTORC1-dependent manner. Cancer Cell. Oct 2006;10(4):269-80.
38. Peng XD, Xu PZ, Chen ML, Hahn-Windgassen A, Skeen J, Jacobs J, et al. Dwarfism, impaired skin development, skeletal muscle atrophy, delayed bone development, and impeded adipogenesis in mice lacking Akt1 and Akt2. Genes Dev. Jun 1 2003;17(11):1352-65.
39. Nawroth R, Stellwagen F, Schulz WA, Stoehr R, Hartmann A, Krause BJ, et al. S6K1 and 4E-BP1 are independent regulated and control cellular growth in bladder cancer. PLoS One. 2011;6(11):e27509.

40. Beggs HE, Schahin-Reed D, Zang K, Goebbels S, Nave KA, Gorski J, et al. FAK deficiency in cells contributing to the basal lamina results in cortical abnormalities resembling congenital muscular dystrophies. Neuron. Oct 30 2003;40(3):501-14.
41. Schlaepfer DD, Hauck CR, Sieg DJ. Signaling through focal adhesion kinase. Prog Biophys Mol Biol. 1999;71(3-4):435-78. Epub 1999/06/04.
42. Hsiao YH, Huang YT, Hung CY, Kuo TC, Luo FJ, Yuan TC. PYK2 via S6K1 regulates the function of androgen receptors and the growth of prostate cancer cells. Endocr Relat Cancer. Aug 2016;23(8):651-63.

Figure Legends:

Figure 1. *Fak* deletion in *Dermo1*-expressing cells leads to osteopenia in mice. MicroCT analysis were performed in femurs of 2-month-old male *Fak*$^{flox/flox}$ (Control), *Fak*$^{flox/+}$;*Dermo1-Cre* (CHet) and *Fak*$^{flox/flox}$;*Dermo1-Cre* (CKO^{Dermo1}) mice. (A-E) Femoral trabecular bone: (A) Representative microCT image, scale bar=500 μm; (B) BV/TV, bone volume fraction; (C) Tb.N, trabecular number; (D) Tb.Th, trabecular thickness; (E) Tb.Sp, trabecular spacing. (F-J) Femoral cortical bone: (F) Representative microCT image, scale bar=300 μm; (G) Tt.Ar, total cross-sectional area inside the periosteal envelope; (H) Ma.Ar, marrow area; (I) Ct.Ar, cortical bone area; (J) Ct.Th, average cortical thickness. Values were presented as median and interquartile range (n=8 for control group, n=9 for CHet group, and n=9 for CKO^{Dermo1} group).

Figure 2. *Fak* deletion in *Dermo1*-expressing cells leads to decreased osteoblast number. Histomorphometric analysis was performed in femurs of 2-month-old male *Fak*$^{flox/flox}$ (Control), *Fak*$^{flox/+}$;*Dermo1-Cre* (CHet) and *Fak*$^{flox/flox}$;*Dermo1-Cre* (CKO^{Dermo1}) mice. (A) Representative

histological image, scale bar=0.7 mm. (B) BA/TA, bone area per tissue area. (C) Tb.N, trabecular number. (D) Tb.Th, trabecular thickness. (E) Tb.Sp, trabecular spacing. (F) N.Ob/BS, osteoblast number per bone surface. (G) Ob.S/BS, osteoblast surface per bone surface. (H) N.Oc/BS, osteoclast number per bone surface. (I) Oc.S/BS, osteoclast surface per bone surface. Values were presented as median and interquartile range (n=7 for control group, n=9 for CHet group, and n=7 for CKO^{Dermo1} group).

Figure 3. ***Fak*** **deletion in** ***Dermo1*****-expressing cells leads to decreased BMSC proliferation.** (A-B) Analysis of percentage of RFP-positive cells in clonal BMSCs isolated from CHet-RFP and CKO^{Dermo1}-RFP mice: (A) Representative fluorescent images. Red indicates RFP-positive signal and blue (Dapi staining) indicates nucleus. Scale bar=100 μm; (B) Quantification of the percentage of RFP-positive cells in day 7 culture illustrated in (A). Data were the average of 6 independent experiments. (C-D) Analysis of Ki67-positive cells in the population of RFP-positive clonal BMSCs isolated from CHet-RFP and CKO^{Dermo1}-RFP mice: (C) Representative fluorescent images in day 3 (D3) and day 7 (D7) cultures. Yellow arrows indicate the $RFP^{+}Ki67^{+}DAPI^{+}$cells; red arrows indicate the $RFP^{+}Ki67^{-}DAPI^{+}$cells; green arrows indicate the $RFP^{-}Ki67^{+}DAPI^{+}$cells. Scale bar=20 μm; (D) Quantification of the percentage of Ki67 and RFP double positive cells illustrated in (C) (n=3). (E) Quantification of the cell number cultured for 3 and 7 days in the same culture system as (C) (n=5). (F-H) CFU-F (colony forming unit-fibroblast) assay of control and CKO^{Dermo1} BMSCs: (F) Representative image of crystal violet staining at day 10; (G) Quantification of the

CFU-F number; and (H) Quantification of the CFU-F size described in (F) (n=4). Each data point represents the average of one independent experiment. Values were presented as median and interquartile range.

Figure 4. FAK kinase inhibition leads to decreased BMSC proliferation. (A) Representative western blot image showing that phospho-FAK (p-FAK) level in BMSCs was dose-dependently suppressed by FAK kinase inhibitor PF-573,228. (B) Quantification of the p-FAK relative level in controls (no treatment and vehicle treatment) and FAK inhibitor-treated BMSCs. p-FAK was normalized to total FAK protein (n=3). (C) Representative fluorescent images of BMSCs isolated from CHet-RFP mice after the treatment with vehicle or FAK inhibitor PF-573,228 for 7 days. Yellow arrows indicate the $RFP^{+}Ki67^{+}DAPI^{+}$cells; red arrows indicate the $RFP^{+}Ki67^{-}DAPI^{+}$cells; green arrows indicate the $RFP^{-}Ki67^{+}DAPI^{+}$cells. Scale bar=20 μm. (D) Quantification of the percentage of Ki67 and RFP double positive cells in the cultures described in (C) (n=3). (E) Quantification of the total cell number in the cultures described in (C) (n=3). (F) Representative image of crystal violet staining in BMSC culture treated with indicated doses of FAK inhibitor PF-573,228 for 10 days. (G) Quantification of the CFU-F number; and (H) Quantification of the CFU-F size in cultures described in (F). Each data point represents the average of one independent experiment (n=5). Values were presented as median and interquartile range.

Figure 5. *Fak* deficiency in osteoprogenitor cells leads to decreased mTORC1 signaling. (A-B) BMSCs isolated from CHet and CKO^{Dermo1} mice were analyzed by western blot: (A)

Representative western blot images using indicated antibodies. (B) Quantification of the relative level of signaling molecules illustrated in (A) (n=5). FAK and β-catenin were normalized to Vinculin and phospho-proteins were normalized to the respective total proteins. (C-D) BMSCs isolated from CHet-RFP and CKO^{Dermo1}-RFP mice were analyzed by immunofluorescence using anti-p-S6 antibody: (C) Representative fluorescent image in day 7 culture. Yellow arrows indicate the $RFP^{+}p\text{-}S6^{+}DAPI^{+}$cells; red arrows indicate the $RFP^{+}p\text{-}S6^{-}DAPI^{+}$cells; green arrows indicate the $p\text{-}S6^{-}Ki67^{+}DAPI^{+}$cells. Scale bar=100 μm. (D) Quantification of percentage of the p-S6 and RFP double positive cells illustrated in (C) (n=3). Values were presented as median and interquartile range.

Figure 6. *Fak* deletion in osteoblasts does not affect bone development. (A) FAK and phospho-PYK2 (p-PYK2) protein levels were analyzed by western blot in cortical bone isolated from femur and tibia of 1-month-old $Fak^{flox/flox}$ (Control) and $Fak^{flox/flox}$;*Col3.6-Cre* ($CKO^{Col3.6}$) male mice. (B) Representative image of 7-week-old control and $CKO^{Col3.6}$ mice. (C) Body weight of male control and $CKO^{Col3.6}$ mice at indicated ages (n=16, 26, 22, 17, 10, 6 in 1 week, 2 weeks, 3 weeks, 4 weeks, 7 weeks and 6 months groups respectively for control mice; and n=22, 34, 23, 17, 9, 8 in 1 week, 2 weeks, 3 weeks, 4 weeks, 7 weeks and 6 months groups respectively for $CKO^{Col3.6}$ mice). (D) Body length of 7-week-old male control and $CKO^{Col3.6}$ mice (n=14 for control mice, n=10 for $CKO^{Col3.6}$ mice). (E-L) MicroCT analysis of femoral trabecular and cortical bone in 2-month-old (2M) and 6-month-old (6M) male mice: (E) BV/TV, bone volume fraction; (F) Tb.N, trabecular

number; (G) Tb.Th, trabecular thickness; (H) Tb.Sp, trabecular spacing; (I) Ct.Th, average cortical thickness; (J) Ct.Ar, cortical bone area; (K) Ec.Pm, endocortical perimeter; (L) Ps.Pm, periosteal perimeter (n=15 and 5 in 2M and 6M groups respectively for control mice, n=16 and 8 in 2M and 6M groups respectively for $CKO^{Col3.6}$ mice). Values were presented as median and interquartile range.

Figure 7. *Fak* deletion in osteoblasts does not affect proliferation and mTORC1 activity. (A) Representative fluorescent images of Ki67 (green) and Dapi (blue) staining in $Fak^{flox/flox}$ (Control) and $Fak^{flox/flox}$;*Col3.6-Cre* ($CKO^{Col3.6}$) BMSCs after 3 and 7 days culture. Red arrow heads point to the $Ki67^{+}DAPI^{+}$cells. Scale bar=20 μm. (B) Quantification of the percentage of Ki67-positive BMSCs described in (A) (n=3). (C) Quantification of BMSC cell number in the same culture as (A) (n=3). (D) Alkaline phosphatase (ALP) staining was performed after 7 days osteogenic culture of control and $CKO^{Col3.6}$ BMSCs. Image was the representative of 6 independent experiments. (E) Alizarin red (AR) staining was performed after 21 days osteogenic culture of control and $CKO^{Col3.6}$ BMSCs. Image was the representative of 6 independent experiments. (F-G) Western blot was performed on lysates of BMSCs isolated from $Fak^{flox/flox}$ (Control) and $Fak^{flox/flox}$;*Col3.6-Cre* ($CKO^{Col3.6}$) mice: (F) Representative western blot image using indicated antibodies in day 0 (first day after plating) and day 7 cultures; (G) Quantification of the relative protein levels as illustrated in (E). FAK and β-catenin were normalized to Vinculin and phospho-proteins were normalized to the respective total proteins (n=4). Values were presented as median and interquartile range.

Figure 8. FAK kinase inhibition decreases mTORC1 signaling of BMSCs in a cell differentiation stage-dependent manner. (A) Representative images of alkaline phosphatase (ALP) staining at indicated days of culture (n=3). (B) Cartoon showing the experimental design of FAK inhibitor PF-573,228 treatment used in (C-D). Dashed red line represented no treatment, dashed black line represented vehicle treatment and solid black line represented 1 μM FAK inhibitor PF-573,228 treatment at indicated culture time in different groups. There were two cohorts of culture: 7 days culture and 11 days culture. In cohort I, D1-D7 means FAK inhibitor was added from day 1 to day 7; D1-D3 means FAK inhibitor was added from day 1 to day 3; D3-D7 means FAK inhibitor was added from day 3 to day 7. In cohort II, D7-D11 means FAK inhibitor was added from day 7 to day 11. (C) At the end of culture in each cohort, BMSCs were analyzed with indicated antibodies. (D) Quantification of the relative level of the signaling molecules illustrated in Cohort I (n=3). (E) Quantification of the relative level of the signaling molecules illustrated in Cohort II (n=3). Phospho-proteins were normalized to the respective total proteins and β-catenin was normalized to Vinculin. Values were presented as median and interquartile range.

Figure 9. Dual inhibition of FAK kinase and PYK2 kinase decreases mTORC1 signaling of BMSCs at later differentiation stage. (A) Representative western blot image showing that phospho-FAK (p-FAK) and phospho-PYK2 (p-PYK2) levels in BMSCs were dose-dependently suppressed by FAK/PYK2 dual inhibitor PF-562,271. (B-C) Quantification of the relative p-FAK

level (B) and p-PYK2 level (C) illustrated in (A) (n=4). p-FAK and p-PYK2 levels were normalized by their respective total protein levels. (D) Cartoon showing the experimental design of FAK/PYK2 dual inhibitor PF-562,271 treatment used in (E-F). Dashed red line indicates no treatment, dashed black line indicates vehicle treatment and solid black line indicates 1 μM PF-562,271 treatment. D7-D11 means FAK/PYK2 dual inhibitor was added from day 7 to day 11. (E) BMSCs were collected at day 11 and extracted proteins were analyzed by western blot using indicated antibodies. (F) Quantification of the relative protein level illustrated in (E). Phospho-proteins were normalized to the respective total proteins and β-catenin was normalized to Vinculin (n=3). Values were presented as median and interquartile range.

Figure 10. Schematic model of the differential roles of FAK in the cells of osteoblast lineage. The model depicts the mechanisms of FAK action at three distinct stages of osteoblast lineage in which the roles of FAK have been addressed by genetic and pharmacological approaches as well as the respective *Cre* transgenes used to target *Fak*, including *Dermo1-Cre* (this study), *Osterix-Cre*,[10] *Col3.6-Cre* (this study) and *Col2.3-Cre*.[9] Red ↔ indicates that the loss of FAK in osteoblasts can be compensated by the upregulated active PYK2.

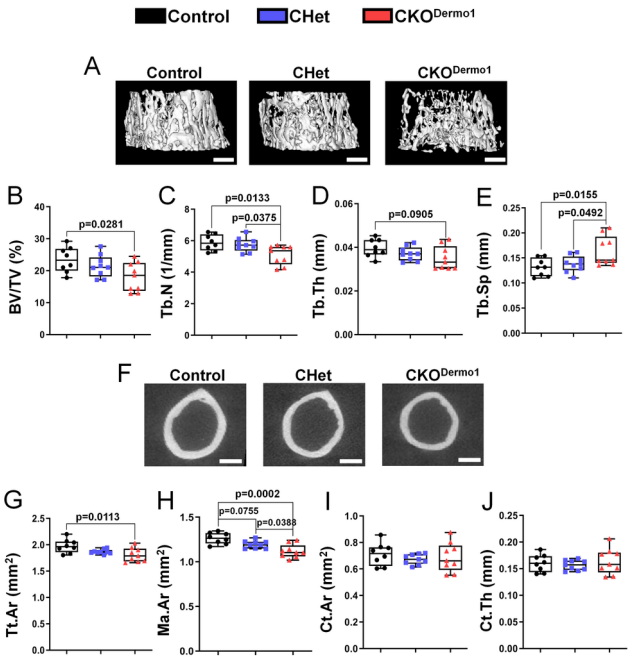

JBMR_4029_Figure 1.tif

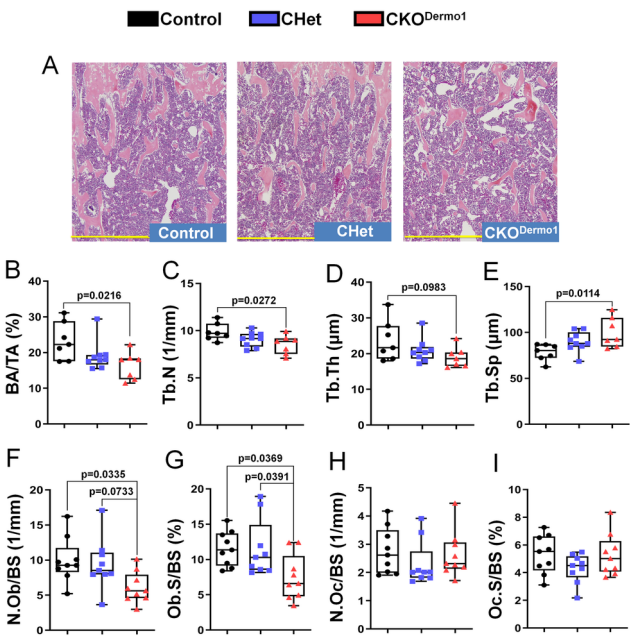

JBMR_4029_Figure 2.tif

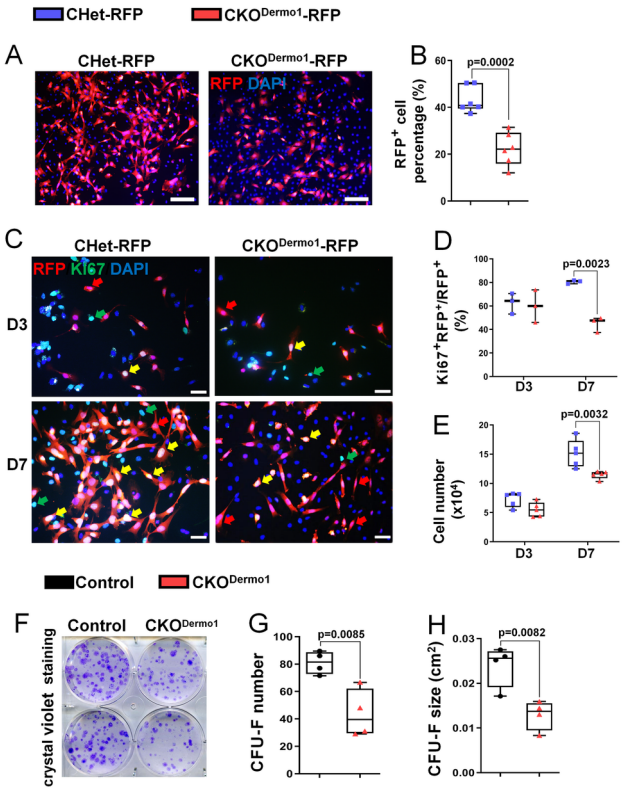

JBMR_4029_Figure 3.tif

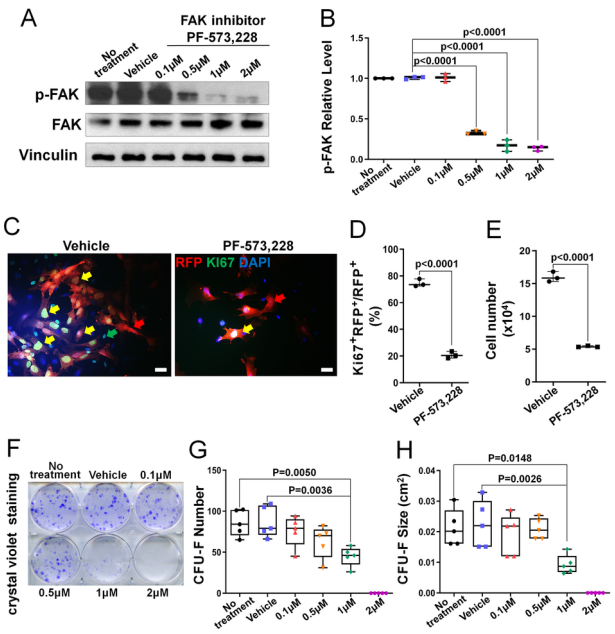

JBMR_4029_Figure 4.tif

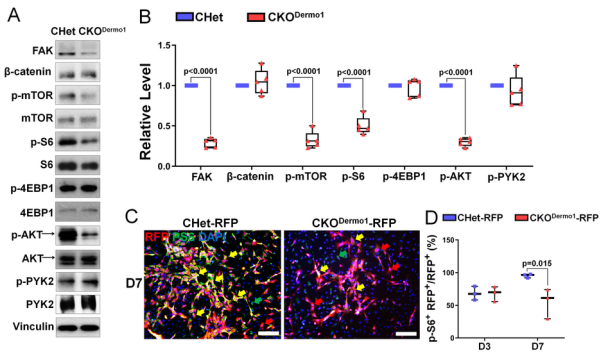

JBMR_4029_Figure 5.tif

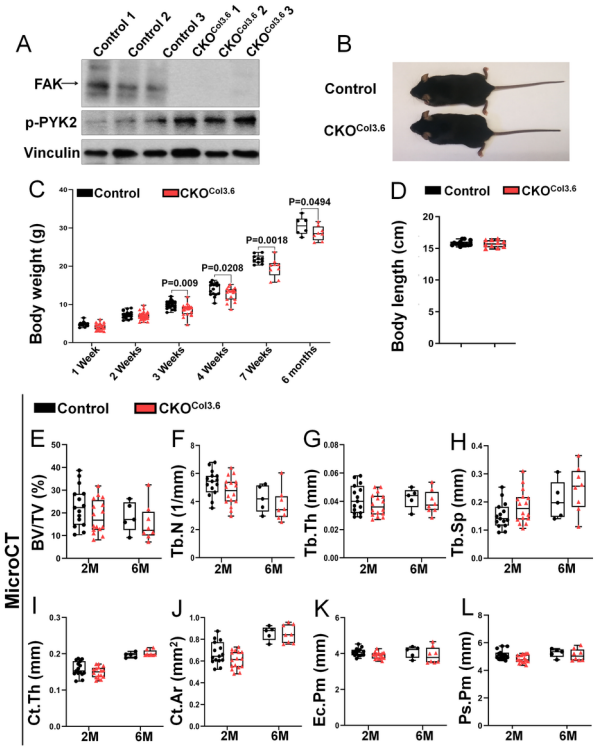

JBMR_4029_Figure 6 20200312.tif

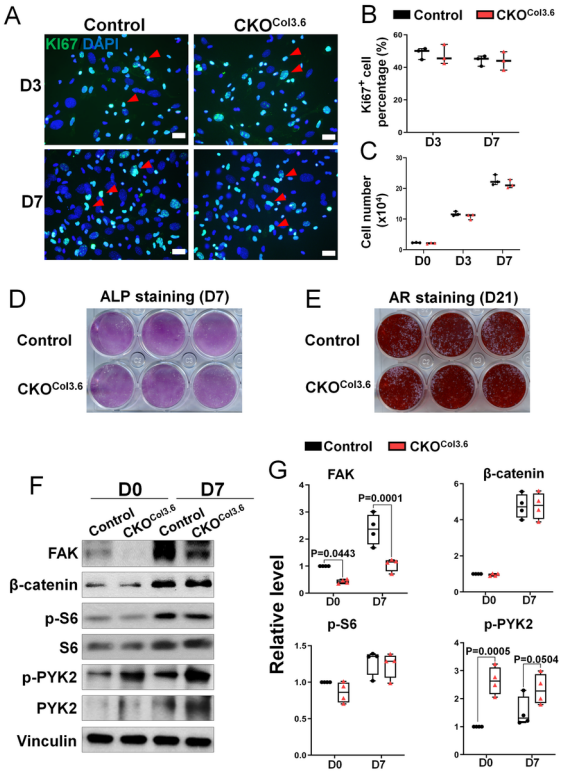

JBMR_4029_Figure 7 20200312.tif

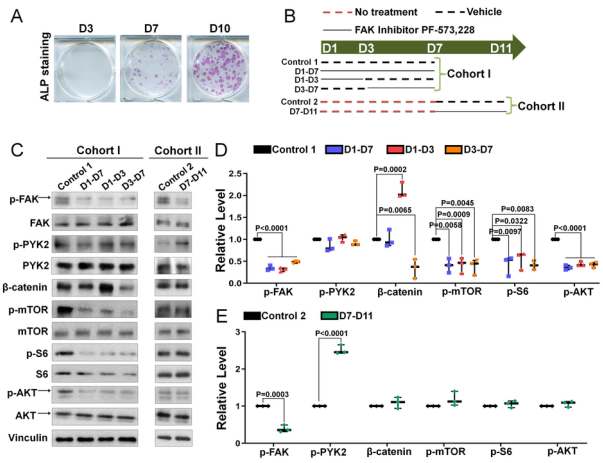

JBMR_4029_Figure 8.tif

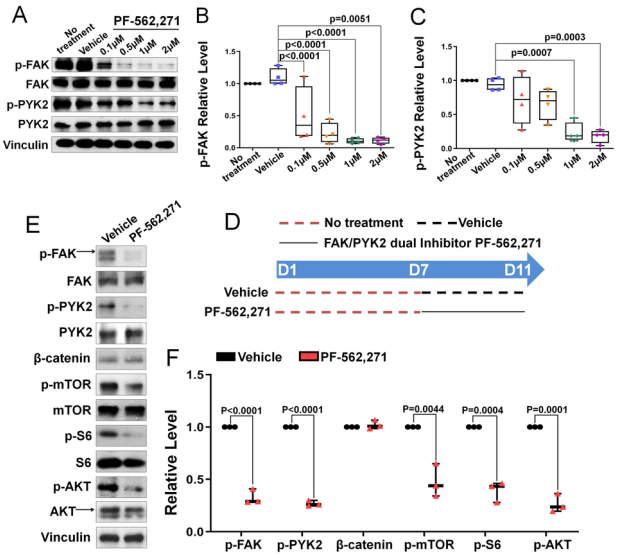

JBMR_4029_Figure 9.tif

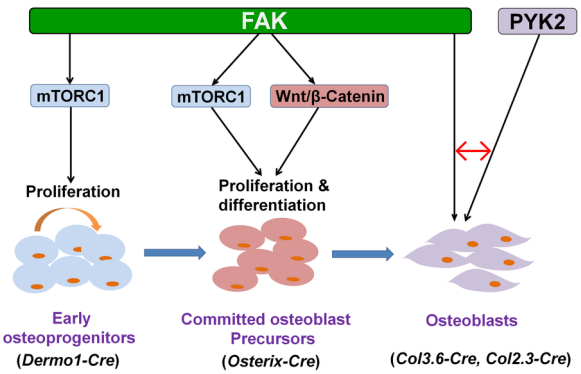

JBMR_4029_Figure 10.tif

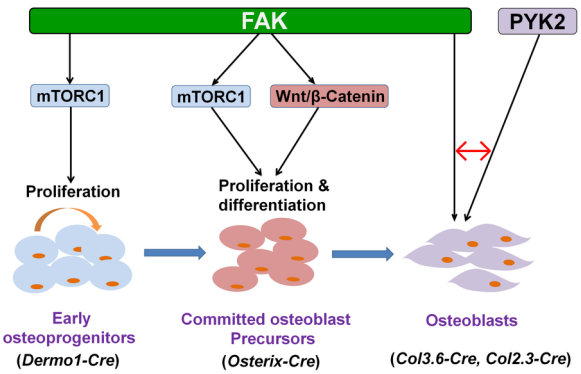

JBMR_4029_graphic abstract.tif